# Unambiguous Dynamic Diffraction Patterns for 3D Depth Profile Measurement

Dominik Lubeley

Communication Technology Institute
University of Dortmund
Germany

**Abstract.** The projection of fixed patterns in active 3d measurement systems is deteriorated by ambient lighting. Moreover classic projection patterns lead to ambiguities during pattern detection in the digital signal processing phase. Therefore a dynamic, diffraction based pattern projection system is introduced which can adapt to ambient lighting conditions. For error-free laser pattern detection a method for the design of unambiguous projection patterns is presented.

## 1 Introduction

Active optical 3d measurement systems use pattern projection for triangulating depth profiles of textureless objects or scenes. In situations with low ambient lighting, structured light approaches like gray code projections with additional phase shift can be used which illuminate the whole measurement space with incoherent light. The pattern contrast is reduced in situations with stronger ambient lighting. In order to improve the performance coherent laser projectors can be used which are capable of bundling their intensity by diffraction – if they are based on dynamic diffraction gratings. This paper describes the generation of arbitrary laser patterns based on a Liquid Crystal on Silicon (LCoS) microdisplay used as a dynamic phase grating. Having the opportunity to generate arbitrary laser patterns, an algorithm for the creation of unambiguous patterns is presented. In contrast to normal evenly spaced patterns, every point can be detected and assigned to its correct source without ambiguities, even when occlusion, wrong or missing detections occur.

## 2 Classic Triangulation

Laser patterns for 3d measurement can be realized with a laser projector either based on geometrical optics using mirrors for beam redirection or wave optics for beam diffraction. While redirection is based on temporally intensity modulation of the total pattern – like line by line scanning, complex phase modulated diffraction patterns are displayed simultaneously.

To use either projection method in conjunction with a camera for depth profile measurement the system has to be calibrated for example by using the algorithm

F.A. Hamprecht, C. Schnörr, and B. Jähne (Eds.): DAGM 2007, LNCS 4713, pp. 42–51, 2007.

presented by Zhang [1]. The extrinsic parameters position and orientation as well as the intrinsic parameters focal length and distortion have to be determined. While this is a typical procedure for camera calibration, the projector has first to be modelled as an inverse camera.

With known geometry the whole triangulation process uses vector algebra. Pattern points are modelled as straight lines

$$\mathbf{x}_{3\mathrm{d}} = \mathbf{x}_{P,0} + r\mathbf{x}_{\mathrm{Ray}} \tag{1}$$

originating from the optical centre $\mathbf{x}_{P,0}$ of the projector, whereas lines in the pattern are planes in the object space.

Centres of pattern points are detected using Gaussian fitting over several pixels in the camera image. The corresponding ray is assigned by selecting the 2d projection of the 3d straight line with the minimum distance to the detected centre.

### 2.1 Classic Patterns

Typical patterns for laser projections are lines or dot structures. Since lines consume much laser intensity and cannot be used for 2d depth profiles in one measuring process this paper concentrates on discrete dot structures which can be projected by the LCoS based spatial light modulator (SLM).

Typical diffraction gratings use a fixed phase distribution with structure sizes in the nanometre range on a glass substrate. With their fixed phase function they project a fixed diffraction pattern, for example $19 \times 19$ points with constant inter beam angle. The fixed grating cannot adapt to different lighting conditions and even worse: Most patterns do not allow an unambiguous detection as described in Sect. 4.

## 3 LCoS Microdisplays as Dynamic Phase Gratings

Switching from static phase gratings to a SLM, diffraction patterns can be projected dynamically. Since amplitude gratings have little diffraction efficiency, a phase grating based on a HD-LCoS microdisplay with high fill ratio was used for high efficiency. To project an intensity distribution of $I(u,v) = |G(u,v)|^2$ the corresponding phase distribution $\phi(x,y)$ with values between 0 and $2\pi$ can be calculated. Input laser plane $g(x,y)$ and diffraction pattern plane $G(u,v)$ are mathematically linked through the diffraction grating with phase shift $e^{j\phi(x,y)}$ by a Fourier transformation in the Fraunhofer region [4]:

$$G(u,v) = |G(u,v)|e^{j\phi(u,v)} = \mathcal{F}\{g(x,y)\} = \mathcal{F}\{|g(x,y)|e^{j\phi(x,y)}\} \ . \tag{2}$$

Therefore the phase distribution can be calculated using an iterative Fourier transform approach as described in [2,3].

As an example for a classical triangulation pattern an $18 \times 18$ dot matrix is depicted in Fig. 1 with the calculated phase distribution according to [2] and the measured intensity of the laser pattern.

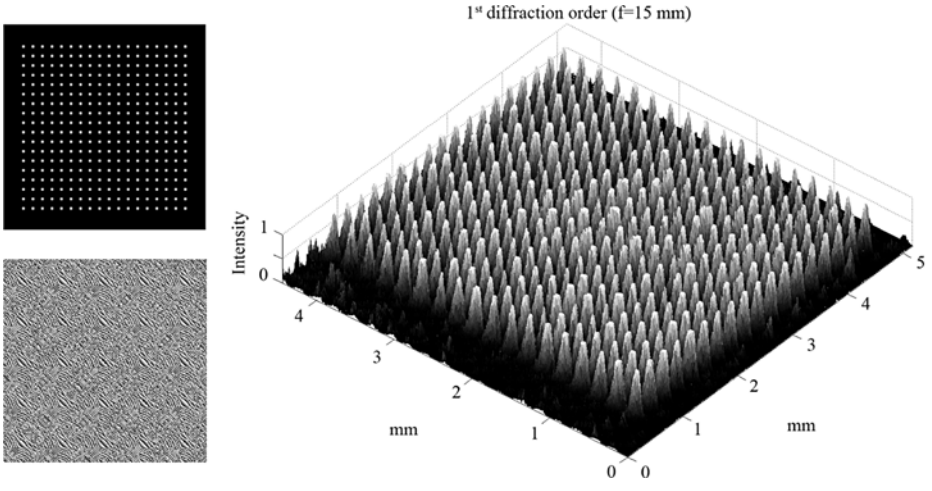


**Fig. 1.** Blueprint of 18 × 18 pattern (top left), phase distribution (bottom left), measured intensity of 1st diffraction order (right)

## 4 Unambiguous Patterns for Error Free Triangulation

To understand the ambiguity of triangulation patterns the projector and camera geometry in object space is shown in Fig. 2. An easy case with the projector centred above the camera with just a x-axis rotation is sketched without loss of generality. The projection pattern is a 3 × 3 dot matrix with constant inter beam angle. The intersections of each ray with the object space as well as their projections on the border of the image space are marked. Each 3d ray (1) can be projected to a 2d line

$$\mathbf{x}_{2\mathrm{D}} = \mathbf{P}\mathbf{x}_{3\mathrm{D}} z^{-1} \tag{3}$$

in the 2d image space which passes through its projected border point, the entrance into the image space.

Remembering epipolar geometry of multiview systems [5] the projector can be regarded as a second, inverse camera. Every projected ray of the projector has an epipolar line in the camera image where its detected reflection can be found. In Fig. 2 the epipolar lines are parallel since their epipol is at infinity in a constellation with the baseline parallel to the image plane. Both camera and projector have the same z-value of zero in camera coordinates. Depending on the projector positioned before ($z > 0$) or behind ($z < 0$) the camera, the epipolar lines are either diverging or converging. Therefore the minimum distance between all epipolar lines is reached either at the border of the image considering divergent lines or at the imaged point of infinity of a ray if the rays are converging. The minimum distance between epipolar lines is named 2d conflict distance within this paper.

If this distance gets too small, detected pattern points cannot be assigned to their corresponding ray. If the distance gets close to zero as for the three spots

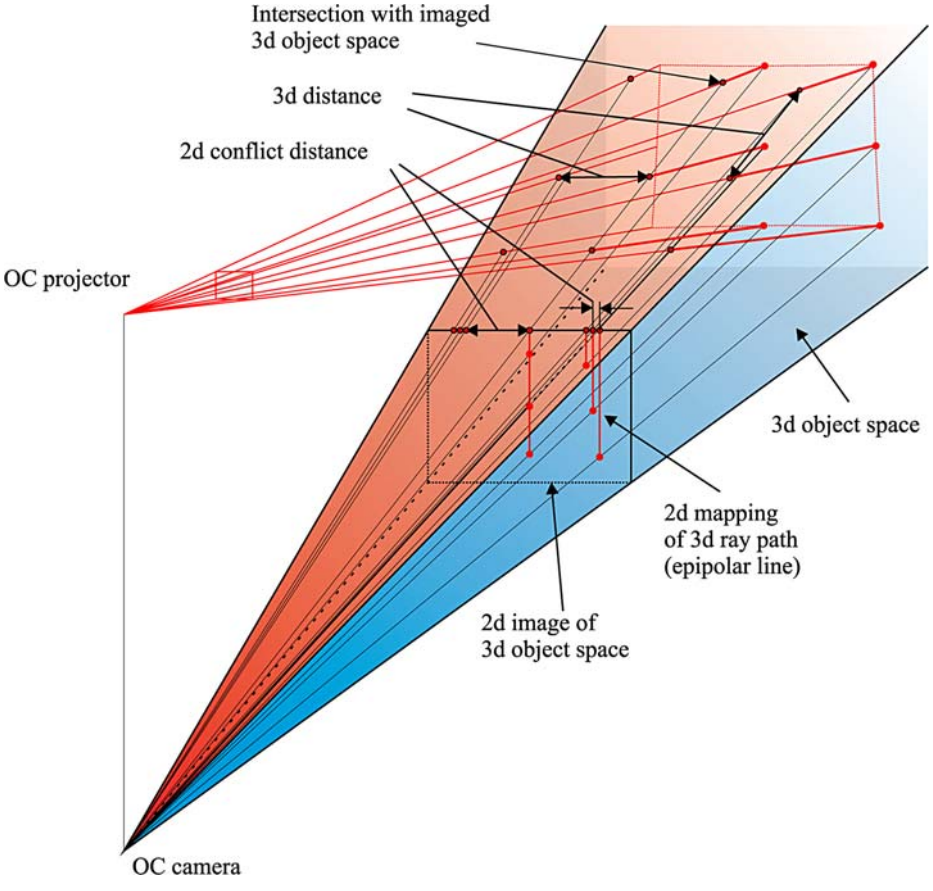


**Fig. 2.** Projection of 3d object space

in the centre column in this example, the situation gets ambiguous. The 3d ray path in object space has the same 2d projection for all three lines. Solving the correspondence problem for these three lines is impossible, if only one pattern point was not detected due to occlusion or contrast problems.

In bigger projection patterns this effect can escalate and corrupt lots of sample points, not only of the same column or row if the orientation between projector and camera changes to a slightly more complex setup.

Knowing the intrinsic matrix of a projector

$$\mathbf{K}_P = \begin{bmatrix} f_x & 0 & c_x \\ 0 & f_y & c_y \\ 0 & 0 & 1 \end{bmatrix} \tag{4}$$

the field of view in both directions can be calculated. In case of the laser projector the field of view can be calculated even easier knowing the illuminating

wavelength $\lambda$ and the structure size $p_{x,y}$ of the pixel elements in the LCoS microdisplay according to

$$\delta_{x,y} = \arcsin\left(\frac{\lambda}{p_{x,y}}\right) \quad . \tag{5}$$

This enables the calculation of the important intersection points of Fig. 2 with all 3d border planes of the imaged object space. Knowing the field of view reveals the border planes' normal vectors

$$\begin{aligned} \mathbf{n}_{\text{right}} &= [-1, 0, \tan(\delta_x/2)]^T & \mathbf{n}_{\text{left}} &= [-1, 0, -\tan(\delta_x/2)]^T \\ \mathbf{n}_{\text{top}} &= [0, 1, -\tan(\delta_y/2)]^T & \mathbf{n}_{\text{bottom}} &= [0, 1, \tan(\delta_y/2)]^T \quad . \end{aligned} \tag{6}$$

The conflict distance in pixel between every ray pair is noted in the conflict distance matrix

$$\mathbf{C}_{\text{Pattern}} = \begin{bmatrix} 0 & a_{21} & a_{31} & \cdots & a_{N1} \\ a_{12} & 0 & a_{32} & \cdots & a_{N2} \\ a_{13} & a_{23} & 0 & \ddots & \vdots \\ \vdots & \vdots & \vdots & \ddots & a_{N(M-1)} \\ a_{1M} & a_{2M} & a_{3M} & a_{(N-1)M} & 0 \end{bmatrix} \quad . \tag{7}$$

This matrix serves as basis for all projection pattern designs. It brands all elements smaller than $d_{\min}$ as conflicting. The sum of all conflicting elements in one column or row indicates the number of conflicts between the corresponding ray and all others. The total cost of one ray is calculated as the sum of all distances of one ray in one column or row

$$c(m) = \frac{1}{\sum_{n=1}^{N} \mathbf{C}_{\text{Pattern}}(n, m)} \quad . \tag{8}$$

### 4.1 Modification of Desired Patterns

Instead of designing new unambiguous patterns a way of modifying desired patterns is introduced.

The total cost function (8) is not appropriate for optimizing the pattern. Rather the conflict distance matrix $\mathbf{C}_{\text{Positions}}$ for all possible ray positions has to be calculated. Having a spatial light modulator for beam diffraction or a step motor positioned mirror for beam redirection in mind, there exist $N$ discrete horizontal and $M$ discrete vertical positions forming a total of $N \cdot M$ possible ray positions. $\mathbf{C}_{\text{Positions}}$ thus consists of $2(N \cdot M)^2$ elements.

With $\mathbf{C}_{\text{Pattern}}$ having conflicting elements smaller than $d_{\min}$, the desired pattern has to be modified. The pattern itself is represented by a pattern matrix $\mathbf{P}$ with dimension $N \times M$ for all possible rays as illustrated in Fig. 1 (top left) and Fig. 4 (top left). As a trivial solution the most conflicting elements with the highest total cost (8) could be deleted. A more refined method is described here.

Within an iterative process, rays are translocated to less conflicting positions, until all conflicts are solved. Only one ray is moved within every iteration cycle.

To decide which ray has to be moved to which neighbouring position, a cost function is computed for each of the $N \cdot M$ possible positions at the start of each iteration. During evaluation the inverse minimum conflict distance

$$c(n,m) = \frac{1}{\min\left(\mathbf{C}_{\text{Positions}}(u,v) | [u,v] \in \text{Patternpoints}\right)} \tag{9}$$

with Patternpoints as the set of indices of active pattern points in $\mathbf{P}$ proved to be a good cost indicator.

Selected rays have to be moved to neighbouring positions with the aim to get a conflict-free, unambiguous projection pattern. Using (9) as the cost indicator, the most conflicting rays have to be moved first. Due to the two competing optimization goals

- pattern conflict avoidance and
- pattern affinity to the desired pattern,

a rating function for neighbouring positions $[n,m]$ compared to the actual position $[n_{\text{actual}}, m_{\text{actual}}]$ within a maximum distance $d_{\max}$ is needed

$$v(n,m) = \frac{c(n,m)/c(n_{\text{actual}}, m_{\text{actual}})}{d} - \mathbf{M}_{\text{Extra}}(n,m) \ . \tag{10}$$

To avoid deadlock situations of rays oscillating between two positions because the surrounding positions are even more expensive, an extra cost memory $\mathbf{M}_{\text{Extra}}$ is introduced. It raises the price of a previous position, when a ray is moved. After a few iterations the ray will leave the deadlock positions, since they get more and more expensive. To prevent wasted positions, the extra cost memory is halved every iteration, so that formerly used positions can be automatically reused after some time – maybe the whole neighbourhood of rays has changed in the meantime leading to a cheap settling position for other rays.

During the iteration the neighbouring position with the best improvement

$$\max(v(n,m) | d < d_{\max}) \tag{11}$$

for the most conflicting ray is selected as the new position and the cost function (9) has to be recalculated.

Always choosing the most conflicting ray can also end up in a deadlock situation, if the ray travels around neighbourhood positions which are all conflicting. They get more extra cost, but with the extra cost being halved every iteration they might be cheap enough for the ray to restart the circle.

First moving other rays away can lead to a better situation for the previously most conflicting ray. Therefore a ray memory $\mathbf{M}_{\text{Ray}}$ is used which adds extra cost to a formerly moved ray – not its position. This memory is also halved every iteration. The rays are sorted according to their cost $c(n,m)$ and indexed. The ray with the highest cost has index 1 at first. With $\mathbf{M}_{\text{Ray}}$ added, the resulting minimum is the index of the ray to be moved next:

$$\text{rayindex} = \min\left(\text{index}(\text{sort}(c(n,m))) + \mathbf{M}_{\text{Ray}}\right) \ . \tag{12}$$

**Fig. 3.** Projection pattern with conflicts

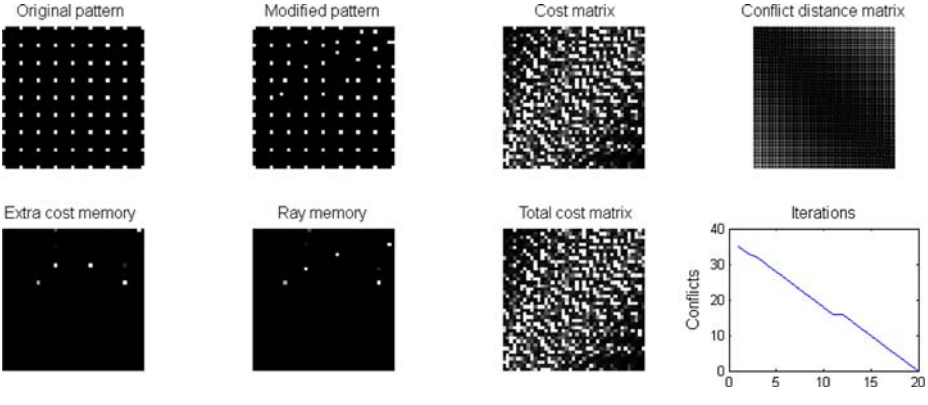


**Fig. 4.** Pattern modification

### 4.2 Simulation Results

To demonstrate the effects of ambiguous and unambiguous patterns, a triangulation setup with given depth map is simulated. The projector is positioned top right of the camera at $\mathbf{x}_{P,0} = [0.1\text{ m}, 0.1\text{ m}, 0\text{ m}]^T$ with an orientation of

**Fig. 5.** Modified projection pattern with specified 5 pixel minimum distance

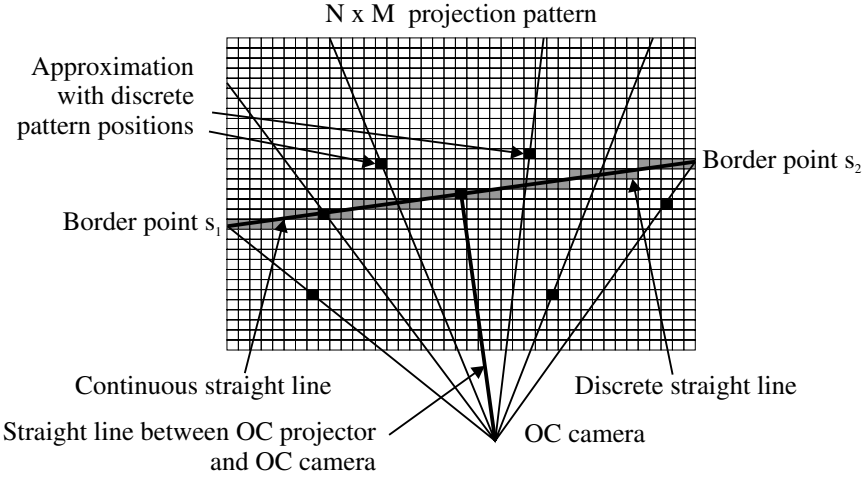


**Fig. 6.** Maximum number of conflict free, discrete rays in the projection pattern matrix

$[-5°, -10°]^T$. As an example a $9 \times 9$ dot pattern with a field of view of 30° is projected into the scene. All ray paths are simulated as well.

In Fig. 3 the ambiguities between ray 18, 41, 64 or 34, 57 and others can be seen. The ray paths are close and even overlapping.

The pattern modification according to Sect. 4.1 is shown in Fig. 4. The original desired pattern $\mathbf{P}$ is at the top left, $\mathbf{C}_{\text{Positions}}$ at the top right, the number of conflicts for every iteration step can be seen at the bottom right, the cost matrix (9) as well as the extra cost memory, total cost matrix and the ray memory after the last iteration step are also visualized.

After 20 iterations the modified pattern is conflict free. A minimum distance of $d_{\min} = 5$ pixel was the preset for this run of the modification algorithm.

As depicted in Fig. 5 the ray paths of the modified, unambiguous projection pattern always keep the preset minimum distance of 5 pixel. No matter where they hit the object plane, the detected dots can be assigned to the correct rays without ambiguities.

### 4.3 Estimation of Parallel Unambiguous Projection Rays

Often it is necessary to know the maximum number of unambiguous rays for a triangulation setup. Knowing extrinsic and intrinsic parameters of projector and camera, the vector $\mathbf{x}_{P,0} - \mathbf{x}_{C,0}$ between the optical centres can be calculated. The straight 2d line in the pattern matrix $\mathbf{P}$ in Fig. 6 which is orthogonal to this vector and passing the image centre, intersects the image border at the positions $s_1$ and $s_2$.

Getting the element $\mathbf{C}_{\text{Positions}}(s_1, s_2)$ reveals the conflict distance from these two rays – the distance between the two entrance points into the 2d image. The maximum number of unambiguous rays

$$n_{\max} = \frac{\mathbf{C}_{\text{Positions}}(s_1, s_2)}{d_{\min}} \tag{13}$$

is only correct for continuous positions on the line between $s_1$ and $s_2$. Although the pattern matrix $\mathbf{P}$ only offers $N \times M$ discrete positions, continuous positions on the line can be approximated with discrete pattern points beside it, verifying this estimation even for patterns with discrete positions. In Fig. 6, $n_{\max}$ is seven.

## 5 Conclusion

In situations with high or varying ambient lighting, projection patterns for triangulation based depth profile measurement need to be changed adaptively. A way for the dynamic generation and projection was introduced: iterative Fourier transform algorithms enable the calculation of phase distributions for a LCoS based dynamic phase grating used for the projection of desired diffraction patterns.

The ambiguity of classic projection patterns which leads to assignment problems between recognized pattern spots and corresponding projection rays in the signal processing phase is described. An algorithm for modifying desired projection patterns to eliminate ambiguities is introduced, which enables an assignment process without critical plausibility decisions – occlusions, wrong or missing detections have no influence.

The proposed projection patterns are not bound to diffraction based laser projections but can be applied to any kind of projection from conventional incoherent up to temporally triggered pattern projectors.

## Acknowledgment

The author thanks the 'Deutsche Forschungsgemeinschaft' (DFG) which funded the presented researches as part of the DFG project 'Optische Tiefenprofilbestimmung auf der Basis adaptiv generierter Beugungsmuster' (KA 1697/4-1).

## References

1. Zhang, Z.Y.: A Flexible New Technique For Camera Calibration. IEEE Transactions on Pattern Analysis and Machine Intelligence 22, 1330–1334 (2000)
2. Lubeley, D.: Laserprojektion auf Basis von Beugung – Bildwiedergabe und 3D-Erfassung. ITG-Fachbericht 199, Vorträge des 12. Dortmunder Fernsehseminars vom 20. bis 21. März 2007 in Dortmund, VDE-Verlag, pp. 197–200 (2007)
3. Fienup, J.R.: Phase Retrieval Algorithms – a Comparison. Applied Optics 21, 2758–2769 (1982)
4. Goodman, J.W.: Introduction to Fourier Optics, 3rd edn. Roberts & Co. Publishers, Englewood, Colo (2005)
5. Schreer, O., Kauff, P., Sikora, T.: 3D Videocommunication: Algorithms, Concepts and Real-Time Systems in Human Centred Communication. pp. 97–101, Chichester [u.a.]: Wiley (2005)